KeAi
CHINESE ROOTS
GLOBAL IMPACT

Available online at www.sciencedirect.com

ScienceDirect

Advances in Climate Change Research 14 (2023) 479–491

www.keaipublishing.com/en/journals/accr/

Numerical optimization on differential adjusting measures for asymmetrical degenerated warm permafrost railway embankment

Yan-Dong HOU[a,b,*], Wen-Yuan LEI[a], Shu-Hao LIANG[a], Ming-Li ZHANG[a,b], Feng-Xi ZHOU[a,b]

[a] *School of Civil Engineering, Lanzhou University of Technology, Lanzhou 730050, China*
[b] *Key Laboratory of Disaster Prevention and Mitigation in Civil Engineering of Gansu Province, Lanzhou University of Technology, Lanzhou 730050, China*

Received 8 February 2023; revised 15 April 2023; accepted 28 May 2023
Available online 2 June 2023

Abstract

Affected by climate warming and shady–sunny slope effect, the permafrost foundation under the railway is undergoing a significant asymmetric degradation process; research on the corresponding regulating or strengthening measures is urgently needed. Based on a well developed of numerical model, we analyzed the 'thermal repair' effect of three redesigned differential thermal reinforcement on the partially degraded permafrost embankment with steps. The results show that, when used as a strengthening measure, the method of laying crushed rock revetment (CRR) with different thicknesses on the sunny and shady slopes cannot completely eliminate the residual warm permafrost regions formed in the previous thermal erosion. When the TCRR scheme is adopted for reinforcement, although horizontal region from the evaporation section of thermosyphones (TPCTs) to the right side of the embankment is remarkably cooled, permafrost under the sunny slope is still deteriorating. In the long run, both ETCRR and TCECRR reinforcement schemes can produce a large range of 'cold core' right below the whole embankment. However, from the perspective of the simultaneous functioning range and cold storage capacity, the TCECRR scheme is signally more efficient. The thermal insulation materials in the above composite strengthening measures can not only resist the heat input in the warm season, but also improve their working efficiency by maintaining the temperature difference between the evaporation section of the heat pipe and the external environment in cold season. The addition of crushed rock revetment in TCECRR has played its thermal semiconductor effect and further improved the comprehensive thermal repair efficiency of the composite measures.

Keywords: Asymmetric degradation; Crushed rock revetment; Thermal insulation materials; TPCT; Reinforcement

1. Introduction

Railway embankment in permafrost areas often carries certain economic, political or even military missions. In the context of global warming, permafrost embankment foundation, especially for those in warm permafrost regions, is suffering from a series of engineering problems caused by the asymmetrical degradation due to the unbalanced solar radiation on two sides of the embankment (Wu et al., 2002; Wen et al., 2010). The previous field monitoring results show that the permafrost foundation with active cooling measures tends to be stable as a whole (Mu et al., 2012; Sun et al., 2018; Wu et al., 2020). However, the field survey and long-period ground temperature and deformation monitoring results show that excessive settlement appeared in some sections of the Qinghai–Tibet Railway (QTR), such as the bridge–subgrade transition sections, general embankment sections of the warm and ice-rich permafrost regions, and high filling subgrades (Qin et al., 2010; Niu et al., 2011). Despite all this, the passive thermal insulation measures to improve the thermal resistance of embankment by raising the height of subgrade or only laying thermal insulation materials are still in use (Ma et al.,

* Corresponding author. School of Civil Engineering, Lanzhou University of Technology, Lanzhou 730050, China.
E-mail address: houyd@lut.edu.cn (HOU Y.-D.).
Peer review under responsibility of National Climate Center (China Meteorological Administration).

https://doi.org/10.1016/j.accre.2023.05.007

2012; Li et al., 2017). With the operation of subgrade, melting interlayer appears in some general embankment sections in warm permafrost areas, resulting in subgrade settlement exceeding 50 cm, and the settlement rate does not slow down (Sun et al., 2018; Wang et al., 2018, 2021). In some sections, although the reinforcement measures of ripped rock revetment was adopted, the reinforcement effect is not ideal due to serious surface ponding or thermokarst lakes (Mu et al., 2018; Peng et al., 2022). What's more, the long-periodic geo-temperature and deformation monitoring data indicate that traditional crushed rock structural embankments are difficult to cope with the thawing or warming of the permafrost foundation under the scenario of 1.5 °C rise in ambient temperature (Wu et al., 2020; Xu et al., 2022). For such linear railways engineering, the occurrence of diseases at any location may lead to paralysis of the whole line. Therefore, it is urgent and necessary to further study the strengthening measures for the potentially unstable sections occurring naturally or during operation of railway with permafrost foundation. Once the best intervention time is missed, a more complicated maintenance process may be confronted in the future.

In order to minimize the thermal disturbance during construction and ensure normal operation during the construction of railway subgrade strengthening project, the controlling measures transversely interspersing the subgrade, such as the ventilation pipe, 'crushed rock sandwich' structure and U-shaped crushed rock structure, will be no longer applicable in the subgrade strengthening project. The combined use of thermal insulation material or crushed rock structures and thermosyphones (TPCTs) is proved by field monitoring data and numerical calculation that it can effectively refreeze and maintain the geo-temperature under the building in a low state for a long time (Hou et al., 2018; Pei et al., 2019a, 2019b; Yan et al., 2020). However, considering the particularity of reinforcement works, for those permafrost foundations that have degenerated with very poor thermal stability, the serviceability of the above and latest proposed measures remains to be further verified. Besides, permafrost foundation below two sides of the embankment slope has been confirmed to have significant differential degradation process under the influence of sunny and shady slope effect (Hou et al., 2022a), especially for which permafrost subgrade built on inclined ground. What's more, in order to shorten the construction period to the greatest extent, reduce the thermal disturbance caused by construction and try not to affect the normal operation of trains during the implement for the reinforcement, excavation should be reduced as much as possible, and the reinforcement measures could be additionally arranged on the exterior of the existing embankment. Therefore, the traditional cooling measures cannot be simply copied and applied to embankment reinforcing engineering. For subgrade strengthening works, the differential design on the sunny and shady side should be carried out considering the above practical factors.

In the above context, we put forward some strengthening schemes and further discussed the comprehensive application effect of TPCTs, thermal insulation material and crushed rock in the differential thermal strengthening on the sunny and shady sides of warm permafrost embankment. The results can provide a scientific basis for the design, construction and future maintenance of permafrost subgrade.

2. Numerical model

2.1. Geometric model

In order to more accurately study the influence of differential reinforcing structure on the service performance of warm permafrost foundation engineering, we took the DK1139 + 940 section of QTR as a prototype, which had been built on a slope and experienced two stages of engineering disposal measures (from 2002 to July 2006, it was a general embankment without any engineering measures (Hou et al., 2022a)). In July 2006, crushed rock revetment shown in Fig. 1a was used for reinforcement paved on the sunny and shady slope surface. To comparatively analyze the strengthening effect of three redesigned reinforcing structures, the overall dimension for embankments in Fig. 2 and the thickness of crushed rock layer in the corresponding different positions are in consistent with Fig. 1a.

We tried to rapidly repair the severe degradation process of the permafrost foundation under it by constantly strengthening the thermal control of the sunny slope of the subgrade, so as to correct the difference between it and the sunny slope of the subgrade. To reduce the weathering effect of the thermal insulation material made of EPS exposed to the external environment and enhance the adhesion of the EPS to the embankment slope, we made a design that fixes the thermal insulation material and the square fiberglass grid with strong weathering resistance through U-shaped anchor as the way shown in Fig. 2b and c, and then fill the square grid with soil. The degradation process of permafrost under the shady slope of subgrade has been detected to be noticeably weaker than that on the sunny slope, and crushed rock revetment laid on the shady slope has been proved to have a good capacity (Mu et al., 2012; Hou et al., 2022a). Therefore, considering the cost of reinforcement engineering, crushed rock revetment is still used as a strengthening measure on the shady slope.

2.2. Heat transfer theory

2.2.1. The coupled air–TPCT–soil heat transfer model

Referring to the previous calculation cases with ideal results (Zhang et al., 2017a; Chen et al., 2018; Pei et al., 2021), we also disassembled the TPCT into three components: evaporation section, thermal insulation section, and the condensation section. Equivalent thermal resistance of each component and the corresponding calculation method is detailed in Table A1.

The length of the condenser, adiabatic, evaporator section (L_c, L_a and L_e), is 1.2, 0.8 and 8.48 m; r_1 and r_2 are the outside diameter of the fins and the smooth pipe, 0.057 and 0.064 m, respectively. The total heat flux Q of the TPCT can be obtained as:

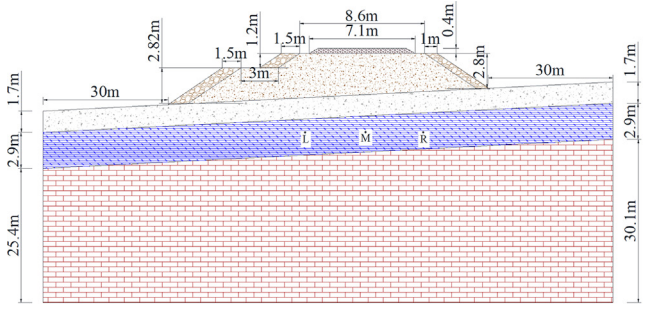

(a) Model size

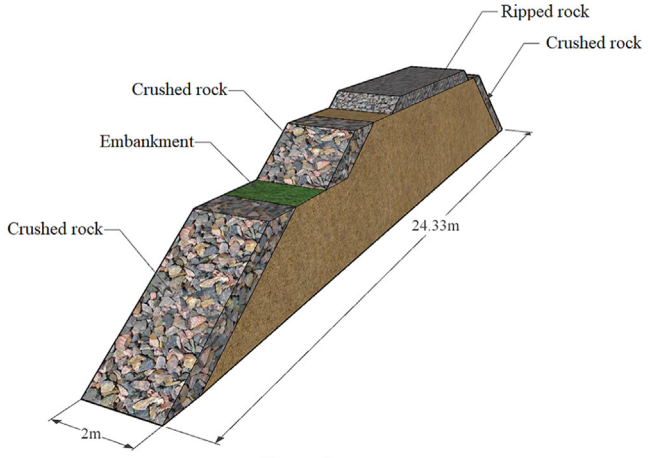

(b) 3D view

Fig. 1. Traditional crushed rock revetment reinforcing structure.

$$Q=\frac{T_a-T_{co}}{R_1}=\frac{T_{co}-T_{ci}}{R_2}=\frac{T_{ci}-T_{el}}{R_3}=\frac{T_{cl}-T_{ei}}{R_4}=\frac{T_{ei}-T_s}{R_5}=\frac{T_a-T_s}{R} \quad (1)$$

where T_a, T_{co}, T_{ci}, T_{el}, T_{cl}, T_{ei} and T_s refer to the temperature of air, tube wall of the condenser, liquid film inside the condenser, liquid film on the inner wall of evaporator, liquid film on the inner wall of condenser, liquid film and liquid pool in the evaporator and soil, among which $T_{el}=T_{cl}$ and $R=\sum_{i=1}^{5}R_i$.

Considering the continuity of heat transfer among the TPCT, air, rock and the soil layers, the coupled heat transfer process of air–TPCTs–rock–soil system can be simplified as:

$$Q=\frac{T_a-T_s}{R}=-\lambda_e\frac{\partial T}{\partial n}\pi d_o l_e \quad (2)$$

Thus, the heat flux density of the contact interface between the evaporation section and the surrounding soil can be calculated as:

$$q_{TPCTs-Soil}=\frac{Q}{\pi d_o l_e} \quad (3)$$

2.2.2. The convection heat transfer model in the crushed-rock or ballast

The heat and mass transfer process in the air domain is described by $k-\varepsilon$ mode. Heat transfer inside the ballast layer and crushed rock revetment is assumed to be the heat and mass transfer process of porous media. The variation process of air density with temperature is calculated by Boussinesq hypothesis. The soil layer region is described by the solid heat transfer equation based on the sensible heat capacity method. Research has shown that when the thermal conductivity between the fluid and solid inside a porous medium is relatively large, there will be a significant temperature difference between the porous medium skeleton and its internal fluid. In this case, the calculation error using the thermal equilibrium model is relatively large (Jiang et al., 1996). The local thermal non equilibrium model can more intuitively describe the convective heat transfer process within the crushed/ripped rock (Hou et al., 2022b), thus improving the accuracy of the calculation of the air-cooled crushed rock structural embankment. Therefore, this article adopts a local thermal non equilibrium model to describe the convective heat transfer process within the rock layer. Under those assumptions, the heat transfer equations of different heat transfer medium domains are listed in Table A2, and the meanings of the parameters involved are given in Table A3.

2.3. Major parameters

The thermal dynamic force parameters of all solid media (including porous media skeleton) and air media involved are shown in Table 1 and Table 2 (Pei et al., 2017; Zhang et al., 2009, 2011).

2.4. Boundary conditions

In a practical situation, the thermal boundary conditions of the embankment and land surfaces can be affected by multiple factors, e.g. superficial budget of solar radiation energy, surface latent heat, climate factors, etc. For the convenience of calculation, the fitted temperature changes are directly applied to the air and engineering component surface (Zhang et al., 2011). Based on 'adherent layer theory' and related references (Yu et al., 2017), simplified temperature variations are given in Eq. 4 and Table 3:

$$T_n=T_0+A\sin\left(\frac{2\pi}{8760}t_h+\frac{\pi}{2}+\alpha_0\right)+\frac{2.6}{50\cdot 8760}t_h \quad (4)$$

where T_0 is the annual averaged surface temperature, T_n is the natural ground surface temperature, A is the annual averaged amplitude of temperature, t_h is the time in hours or days, α_0 is the phase angle which depending on the time of embankment completion time or the time when reinforcement measures are implemented.

We analyzed the effectiveness of three different reinforcement measures taking on the shady and sunny slope to deal with the asymmetric degradation of the underlying permafrost foundation assuming which with a MAGT of −0.65 °C. Referring to previous study (Zhang et al., 2009), the heat flow of the soil layer at the depth of 30 m is about 0.06 W m^{-2}. Symmetrical boundary is adopted on both sides of the soil layer in Fig. 3.

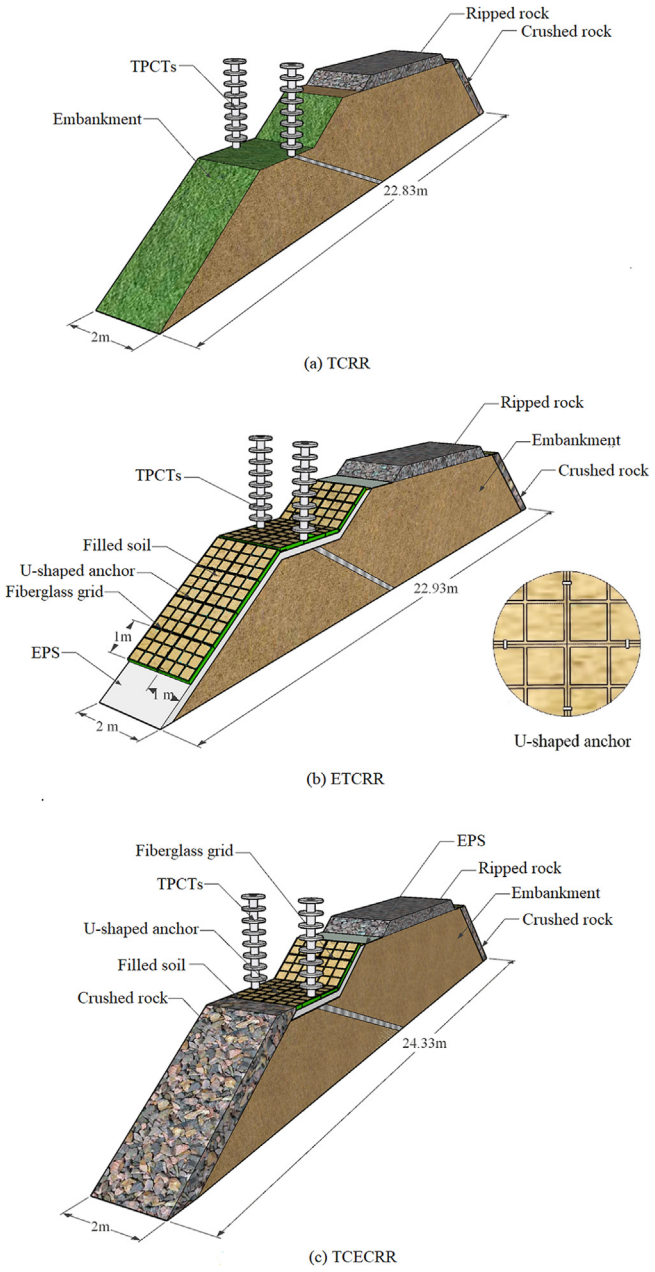

Fig. 2. 3D view for the three redesigned reinforcing structures (CRR, crushed-rock revetment; TCRR, the asymmetric strengthening measures of TPCTs and CRR for sunny slope, and shady embankment slope, respectively; ETCRR, thermal insulation material is additionally used and expanded polystyrene (EPS) is added to the sunny side on the basis of the TCRR scheme; TCECRR means TPCT, EPS, and crushed rock are comprehensively used on the sunny slope of the embankment, and CRR paved on the shady slope is consistent with the other two schemes).

As shown in Fig. 1, the main aggregate size ranges from 18 to 30 cm and from 2 to 5 cm in the crushed rock domain and the ballast region. Permeability and coefficient of inertia resistance can be calculated according to the particle size using the method in Liu et al. (2017). Besides, the heat insulation material (used in new design) thickness is 10 cm.

Based on the latest field data (Zhao et al., 2019), the mean annual wind velocity is 3.64 m s^{-1}. Wind speed of turbulence close to the condenser section of the TPCTs can be expressed as follows (Zhang et al., 2015).

$$V_{10} = 3.64 + 1.10 \times \sin\left(\frac{2\pi t}{8760} + \frac{4\pi}{3} + \alpha_0\right) \quad (5)$$

$$V_h = V_{10}\left(\frac{H}{10}\right)^{0.16} \quad (6)$$

where V_{10} and V_h represent wind velocity at a height of 10 m and h m, H is the height from surface.

2.5. Simulation steps

The numerical simulation is carried out in three stages, as shown in Fig. 3.

Space between two TPCTs in the embankment extending direction is set as 2 m as the long-term experience on QTR. In order to consider the worst situation, all of the thermal field section is sliced in the central place between two TPCT in the longitudinal direction, by the way shown in Fig. 4.

2.6. Numerical analysis method

The coupled air–TPCT–rock–soil model, expressed with the equations in Table 2, is heavily nonlinear, and can only be solved by numerical method. The spatial and temporal discretization of the coupled Eqs. are carried out numerically by the 'control volume integration method'. The discrete equations are solved in an iterative manner using the successive under-relaxation method (Zhang et al., 2017a). Each iteration ends when the normalized variation of solution result is less than 10^{-6} for every time step (Zhang et al., 2017b).

3. Results and analyses

3.1. Evolution of thermal state between different schemes

In order to evaluate the short-term, medium and long-term cooling capacity of the newly proposed strengthening measures on the subgrade and permafrost foundation, we simulated the reinforced subgrade in Figs. 1 and 2 for 30 years. In order to simplify the description below, we have simplified the full name of the above subgrade structure. The strengthening measure of crushed rock revetment protection for both the sunny and shady embankment slopes is simplified to CRR (Fig. 1). The asymmetric strengthening measures of TPCTs and CRR for sunny slope and shady slope of embankment are simplified as TCRR[1] (Fig. 2a). TPCT and thermal insulation materials are used for the sunny slope, and crushed rock revetment is used for the shady slope. Composite measures combining thermal insulation materials and TPCTs are

[1] TCRR, the asymmetric strengthening measures of TPCTs and CRR for sunny slope, and shady embankment slope, respectively.

Table 1
All thermal parameters of solid medium and porous skeleton.

Physical variable	λ_f (W m^{-1} °C^{-1})	C_f (× 10^6 J m^{-3} °C^{-1})	λ_u (W m^{-1} °C^{-1})	C_u (× 10^6 J m^{-3} °C^{-1})	L (× 10^7 J m^{-3})
Crushed and ripped rock	3.000	1.006	3.000	1.006	0.00
Embankment	1.980	1.913	1.919	2.227	2.04
EPS	0.030	1.846	0.030	1.846	0.00
Pebbly sand	1.650	1.825	1.450	2.456	4.14
Sub-clay	1.350	1.879	1.125	2.357	6.03
Strongly weathered mud-stone	1.820	1.846	1.474	2.099	3.77

Note: The embankment is filled with gravel soil. The main components of strongly weathered mud-stone are limestone parent rock in small proportion and its weathered products.

adopted for the sunny slope of the subgrade, and CRR is adopted for the shady slope of the subgrade. This asymmetric enhancement is simplified to ETCRR[2] (Fig. 2b). On the sunny side, the upper slope surface is paved with thermal insulation materials, the lower slope surface is paved with crushed rock revetment, and TPCTs are inserted at an inclined angle at the step. Meanwhile, the shady side of the embankment is strengthened by CRR. This asymmetric strengthening measure is simplified as TCECRR[3] (Fig. 2c).

It can be seen from Fig. 5 that on July 15, after six years of operation, although the 0 °C isoline below the subgrade center migrated up to the original ground surface, a high temperature area of 0–0.5 °C also appeared under the subgrade with a 'thawing core' interlayer. If this phenomenon continues to evolve, it may lead to excessive settlement and a series of secondary problems. Fig. 6 shows the temperature contour map of the above strengthened subgrade structure on 15 January in the 1st, 5th, 8th, 15th and 30th years. The horizontal and vertical axis names of the contour map in the table are 'horizontal position (m)' and 'depth (m)', respectively. The same applies to Figs. 7, 8 and 10 below. It can be seen from Fig. 6 that within 30 years after CRR strengthening, the temperature of the permafrost foundation below the subgrade has been within the range of 0–0.5 °C in cold season. At the same time, from the contour line of 0 °C, there is always a melting interlayer on the sunny side of the subgrade. The scope of the interlayer first shrinks to a local range at the toe of the embankment and then expands to the original permafrost table (PT). In contrast, the contour line of −0.5 °C under the shady slope of the subgrade shows that the temperature near the original natural PT of the shady slope once dropped below −0.5 °C during the 0–15 years after strengthening. This shows that strengthening with CRR alone is not enough to completely eliminate the heat accumulation in the deeper layer of permafrost foundation below the sunny slope during the early operation of the original general subgrade. This also further confirms the conclusion in our other study (Hou et al., 2020). In contrast, the other three schemes of inclined inserting TPCTs can directly cool the soil at the subgrade centerline due to the fact that the heat insulation section of the TPCTs extends directly below the track. When TCRR is used for strengthening, although the cooling effect around the condensation section of the TPCTs is significant, the direct lower part of the sunny slope has always been a thawing state, and the thermal erosion under the sunny slope of the subgrade is still very serious. This may lead to the occurrence of subgrade slope, and the potential sliding threatens the safety of subgrade (Pei et al., 2017). This indicates that further thermal protection measures should be taken at the lower slope of the sunny slope of the subgrade. With the laying of thermal insulation materials on the sunny slope of the subgrade in the ETCRR thermal strengthening measures, the cooling effect near the condensation section of the TPCTs has been remarkably strengthened compared with TCRR, and the earlier heat accumulation right below the sunny slope of the subgrade has also been dissipating with year. This also indirectly indicates that the laying of thermal insulation materials helps to increase the annual accumulation of 'net cold storage' of TPCTs in cold seasons. However, according to the cooling process of the lower soil layer of the sunny slope during the 0–15 years after strengthening, the cooling efficiency of this measure in short term is still not completely satisfactory. In order to further improve the cooling efficiency of the strengthening measures, TCECRR replaced the insulation material laid on the downhill surface of ETCRR's sunny slope with rubble slope protection. It can be seen that under the strengthening of TCECRR, the melting interlayer in the lower part of the sunny slope disappeared in the first year. Compared with the evolution of isolines of −1 and −0.8 °C in ETCRR scheme, the cooling efficiency of TPCTs has been further improved, and its influence scope in both horizontal and vertical directions has expanded to the whole bearing stratum in the 15th–30th years. Permafrost type of the foundation has also changed from high-temperature permafrost to low-temperature permafrost, and the service performance of the project has been dramatically improved.

Fig. 7 shows the evolution process of ground temperature isolines in the 1st, 5th, 8th, 15th and 30th years respectively when CRR, TCRR, ETCRR and TCECRR are strengthened at the maximum annual thawing depth. It can be seen that PT below the sunny slope of the subgrade rises slightly in a small range in the fifth year after CRR scheme is adopted for strengthening, while PT below the subgrade center does not rise markedly. The range between the contour lines of −0.5

[2] ETCRR, thermal insulation material is additionally used and expanded polystyrene (EPS) is added to the sunny side on the basis of the TCRR scheme.
[3] TCECRR means TPCT, EPS, and crushed rock are comprehensively used on the sunny slope of the embankment, and CRR paved on the shady slope is consistent with the other two schemes.

Table 2
Aerodynamic parameters.

Physical parameters	C (kg k)	λ (W (m k) $^{-1}$)	ρ (kg m^{-3})	μ (Pa s)	β
Air	1.004×10^{3}	2.0×10^{-2}	0.641	1.750×10^{-5}	0.00387

and 0 °C in the lower part of the subgrade in 0–15 years is slowly expanding year by year, and the contour lines of −0.5 °C move down apparently in the 30th year with the degradation of the permafrost around the subgrade. This further shows that only CRR scheme can barely maintain the thermal state of the subgrade after thermal disturbance after several years of operation, and cannot completely reverse the degradation process of permafrost foundation caused by thermal disturbance in the earlier stage. From the contour lines of −0.5 and −0.8 °C in the TCRR scheme, although the 'cold energy' accumulated in the cold season near the centerline of the subgrade has not been completely dissipated in the warm season, PT directly below the sunny slope of the subgrade has moved downward year by year, and even exceeded the original natural PT from the fifth year. In the first year after ETCRR scheme is strengthened, PT of permafrost will rise to the original natural surface. With the service time coming to five years, the position of PT is basically stable, and PT below the subgrade center is raised to 2.5 m. In addition, the −0.8 °C area contour below the subgrade center gradually expands over time. In the 30th year after the strengthening, the −0.8 °C isotherm profile was extended to −7.5 m at the lowest, and the thermal stability of the subgrade was prominently improved. However, according to the evolution of the area between the contour lines of −0.5–0 °C, the contraction rate of this area is not ideal within eight years after the use of this measure. The continuous existence of this high temperature zone may lead to a certain soft substratum effect in the foundation soil under the sunny slope of the subgrade, which may not completely alleviate the deformation trend of the subgrade at this stage. At the beginning of service, TCECRR can substantially raise PT of permafrost, with the lowest limit of 0.6 m. With the increase of time, the impact of climate warming on the underlying permafrost of subgrade is not noticeable. After eight years of service, the high-temperature frozen soil under the subgrade begins to show −1 °C isotherm profile, and then gradually expands. In 30 years, the maximum depth of the isotherm profile can reach −8 m, which is extremely beneficial to the thermal stability of the subgrade during service.

Table 3
Parameters involved in Eq. 4.

Variable	T_0 (°C)	
Ambient air	−4.0	12.0
Natural ground surface	−0.6	12.0
Sunny slope surface	1.2	14.0
Shady slope surface	−1.5	15.0
Top of embankment, CRR and RR	1.5	16.0
Mean annual ground temperature (MAGT)	−0.65 °C	

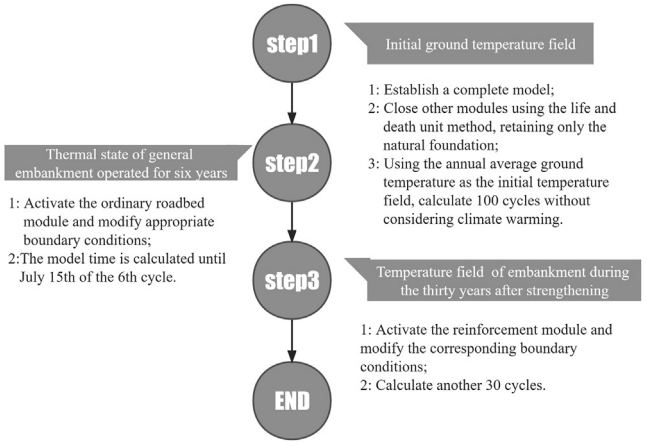

Fig. 3. Numerical calculation process flowchart.

3.2. Thermal state evolution near the original PT under ballast after reinforcement

The thermal state near the original natural PT (especially in the surrounding area of the subgrade center) is closely related to the overall stability of subgrade (Mu et al., 2012). Fig. 8 gives the 30-year ground temperature time history curve of the original PT position on the left (L), middle (M) and right (R) shoulders of the subgrade and directly below the subgrade center after reinforcement, marked in Fig. 1a. On the whole, the subgrade goes through three stages: 1) the warming stage before the measures are taken; 2) the rapid cooling stage after strengthening measures; 3) the geo-temperature rise stage after the strengthening measures exceed the limit cooling capacity under the background of climate warming. From the evolution of the ground temperature time history curve, although there

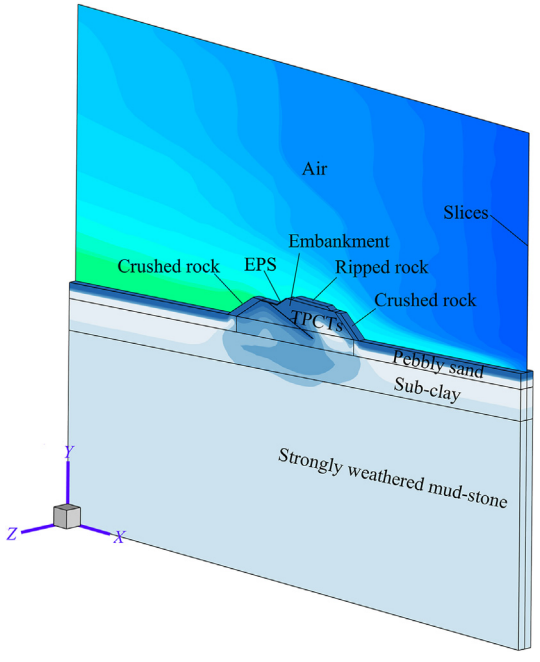

Fig. 4. Target plane sliced from the 3-dimensional model.

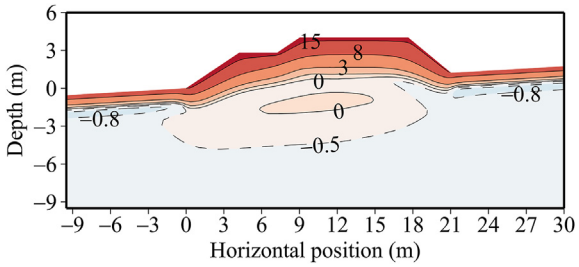

Fig. 5. Thermal regime of general embankment on 15 July which has operated for six years.

was a weak cooling process after the CRR program was strengthened, the original PT from the shoulder of the sunny slope to the central location was always in the 'extremely unstable thermal state of high temperature' higher than −0.5 °C. When the TCRR scheme is adopted for strengthening, the annual minimum ground temperature from the subgrade center to the subgrade shady slope shoulder will drop to −1.5 and −0.9 °C respectively during the 0−15th year period. Although the ground temperature under the shoulder of the sunny slope of the subgrade once dropped to −0.7 °C, the ground temperature began to rise rapidly in the 20th year after strengthening. When ETCRR and TCECRR schemes are adopted for strengthening, a severe cooling process occurred from the shoulder on the sunny slope of the subgrade to the center of the subgrade during the 0−18th years, and the cooling efficiency of the TCECRR scheme under the shoulder on the shady slope of the subgrade is visibly better than that of ETCRR.

3.3. Enthalpy evolution of soil mass after reinforcement

The strengthening measures are mainly to improve the thermal stability of the permafrost subgrade by increasing the input of 'cold energy' in the permafrost foundation under the subgrade in cold season and slowing down the release of cold energy in the soil in warm season. The heat energy in soil at a certain temperature can be calculated by $E = H(T_{\mathrm{ref}}) + \int_{T_{\mathrm{ref}}}^{T} C_{\mathrm{p}}(T)\mathrm{d}T$. Wherein, H (T_{ref}) is the standard enthalpy at the reference temperature, T_{ref} is the reference temperature, and C_{p} is the specific heat. In order to clarify the transformation process of thermal energy in subgrade soil between different strengthening schemes in cold and warm seasons, Figs. 9 and 10 respectively give the contour maps of thermal energy on 15 April and 15 October in the 1st, 5th and 30th years of subgrade and its lower permafrost foundation under the action of four strengthening measures.

From Fig. 9, during the first five years of CRR service, the −50 kJ contour area below the sunny slope of the subgrade gradually changes to −60 kJ area, while the −80 kJ contour envelope area shrinks from the right side of the subgrade to the soil at the sunny slope side. From the −90 kJ contour line, the heat erosion effect of the shady slope side is noticeably weaker than that of the sunny slope side in the early stage, and the lower soil mass shows a further cold storage process in this

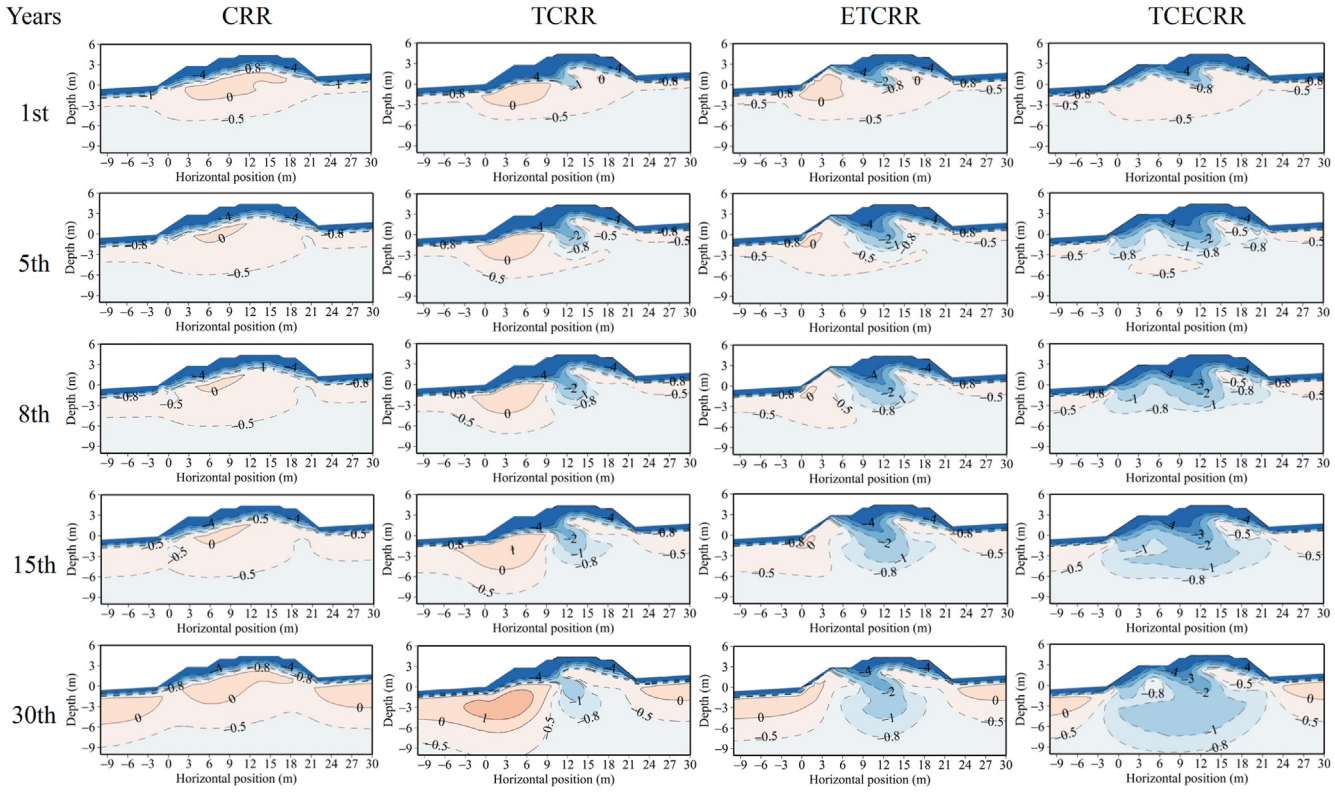

Fig. 6. Thermal regime of the reinforced embankment on 15 January in the 1st, 5th, 8th, 15th and 30th year.

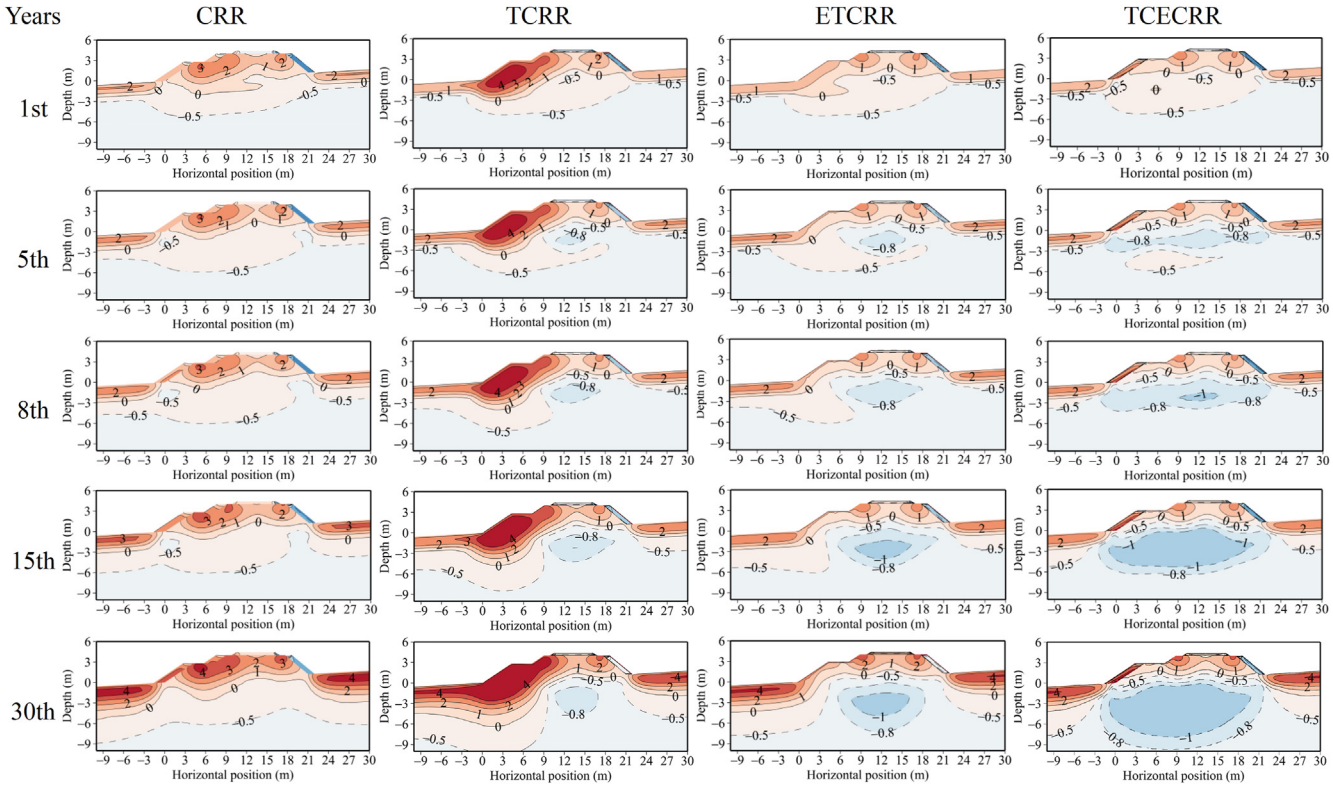

Fig. 7. Thermal regime of the reinforced embankment on 15 October in the 1st, 5th, 8th, 15th and 30th year.

stage. With the continuous warming of the climate, in the 30th year, the −60 kJ energy contour area of the soil mass in the lower part of the sunny slope degenerates to −50 kJ, while the envelope area of −80 and −90 kJ energy contour gradually shrinks downward. This shows that in the process of external warming, the cold storage of the deep permafrost foundation under the sunny slope has been consumed in the medium and long term. In TCRR scheme, the soil mass near the lower evaporation section of the ballast is always in the 'cold storage state' after strengthening, and the maximum thermal energy isoline increases from −90 kJ in the first year to −130 kJ in the 30th year after strengthening, and the area is also further expanding and extending downward. From the −70 kJ contour line, the cold energy of the permafrost foundation below the sunny slope increases slightly in the shallow layer with time, while it continues to decrease in the deep layer. However, after the ETCRR scheme is adopted for strengthening, the cold energy of permafrost directly under the ballast has been in the process of accumulation, and this part of cold energy is gradually diffusing to the two subgrade slopes with the increase of time. This effect also urges the permafrost foundation under the sunny slope to be in the cold energy accumulation state all the time. After strengthening with the TCECRR scheme, the cold energy accumulation process at each position of the embankment or its soil mass is evidently strengthened in depth and width on the basis of the ETCRR scheme. At the same time, the distribution of cold energy in permafrost foundation is more uniform than that in ETCRR scheme.

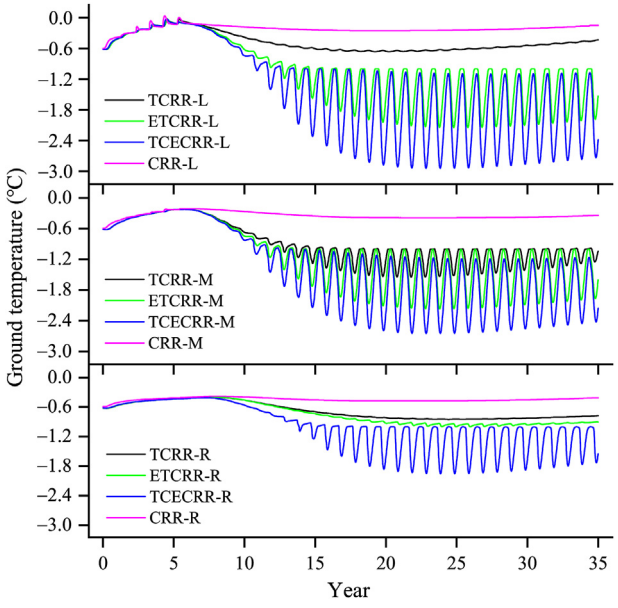

Fig. 8. Temperature time history curve of soil at left (L), middle (M) and right (R) positions marked in Fig. 1 after strengthening with different schemes.

After a warm season, from the thermal energy isoline of −29 and −30 kJ inside the embankment in the same year, the thermal protection capacity of the four strengthening measures in the warm season is in the order of strong to weak: TCECRR > ETCRR > CRR > TCRR (Fig. 10). Compared with the situation in Fig. 9, from the −50 and −70 kJ thermal

energy isolines in the permafrost foundation under the sunny slope, it can also be found that the cold energy dissipation in the permafrost foundation under the TCRR scheme is the most serious. From the isoline of −50 and −70 kJ, the dissipation of cold energy in the foundation soil of the other three schemes in the warm season mainly occurs from the original natural PT to the surface. The cold energy in the area below the original natural PT is almost the same as that on 15 April.

4. Discussion

4.1. Thermal state below the middle subgrade steps on sunny side

Figs. 11 and 12 show the thermal state in the middle of the steps of the sunny slope subgrade on 15 January and 15 October (at the maximum annual thawing depth), in the 1st, 5th and 30th year after strengthening. It can be seen from Fig. 11 that after the TCRR scheme is adopted for strengthening, ground temperature range between 0 and 3 m below the steps of the sunny slope of the subgrade is apparently lower than that in the ETCRR and TCECRR cases. This shows that the natural refreezing process of sunny slope without protective measures is stronger than that of slope protection with thermal insulation materials and crushed rock revetment. During the 1st–5th years after the strengthening of TCRR scheme, the range from −0.5 to −5.8 m was still in a melting state on 15 January, and the artificial PT was not substantially raised. After 30 years of strengthening, although the artificial permafrost has been uplifted to the original natural surface, the melting area has also been expanded to the range of 0–6 m. In the first year after ETCRR is adopted for strengthening, the artificial PT at this location has been raised up to the original natural surface, and 'zero curtain' has occurred within the range of 0 to −1.5 m. In the 5th year after the strengthening, the soil mass has completely the refrozen, in which the maximum cooling amplitude within the range of −1 to −3.5 m is −0.4 °C compared with the first year. During the 30 years after the strengthening, a strong cooling process occurred within the range of 0 to −8 m, and the maximum temperature drop occurs at −2 m with an amplitude of about 0.5 °C. In these three years after the adoption of TCECRR enhancement, the ground temperature change law is similar to that of ETCRR scheme, but the cooling amplitude and range during the 5th–30th years are greater than that of ETCRR. This shows that the thermal protection measures on the superficial sunny slope of the embankment retard the refreezing efficiency of the adjacent soil mass to a certain extent, but this effect does not seem to affect the deep soil layer, but rather strengthens the cooling of the deep soil. The cooperative work of crushed rock revetment, thermal insulation material and inclined TPCTs in TCECRR scheme makes this phenomenon more significant.

As can be seen in Fig. 12, when TCRR strengthening is adopted, the low temperature envelope at this position continues to move towards the high temperature direction, and the artificial PT is also decreasing year by year. However, after ETCRR strengthening, the artificial PT has been rising year by year in these three years, and it remains 1 m above the original natural surface by the 30th year. The ground temperature in the range of −9 to −1 m is decreasing year by year in the above three years. This indicated that thermal disturbance formed during operation without thermal protection measures has been repaired and consolidated year by year. For the above three years, the TCECRR scheme is superior to the ETCRR scheme in terms of both the inter-annual uplifting amplitude of the artificial PT and the cooling range and amplitude of ground temperature.

4.2. Working characteristics at different positions of the evaporation section

Fig. 13 shows the surface heat flux of the evaporation section along the length of the TPCT on 15 January in the 1st, 5th and 30th years (the air temperature reaches the annual minimum) under the three working conditions of TCRR,

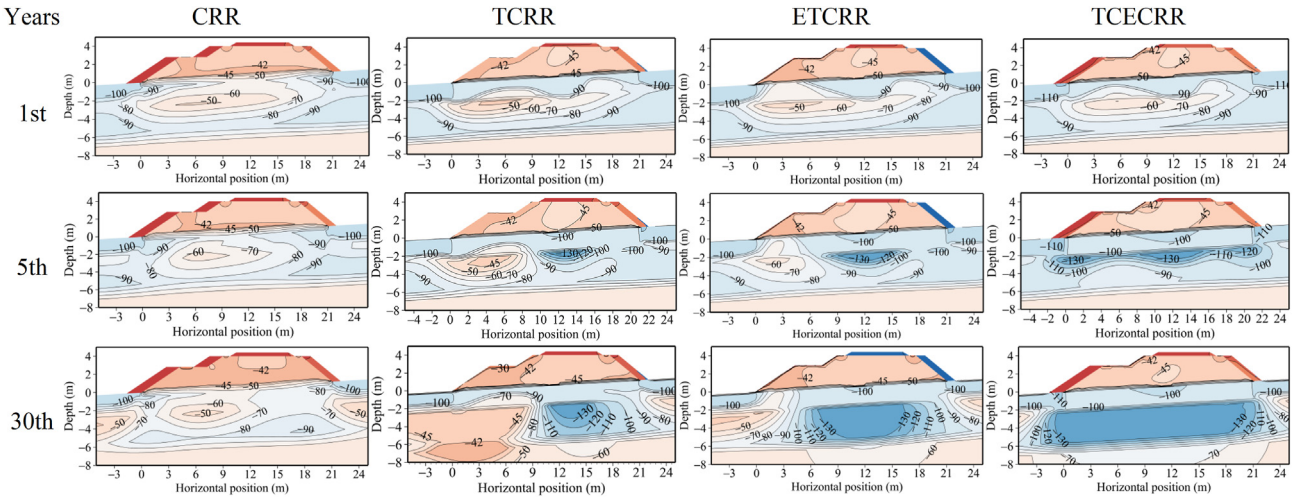

Fig. 9. Enthalpy of the reinforced embankment on 15 April in the 1st, 5th and 30th year.

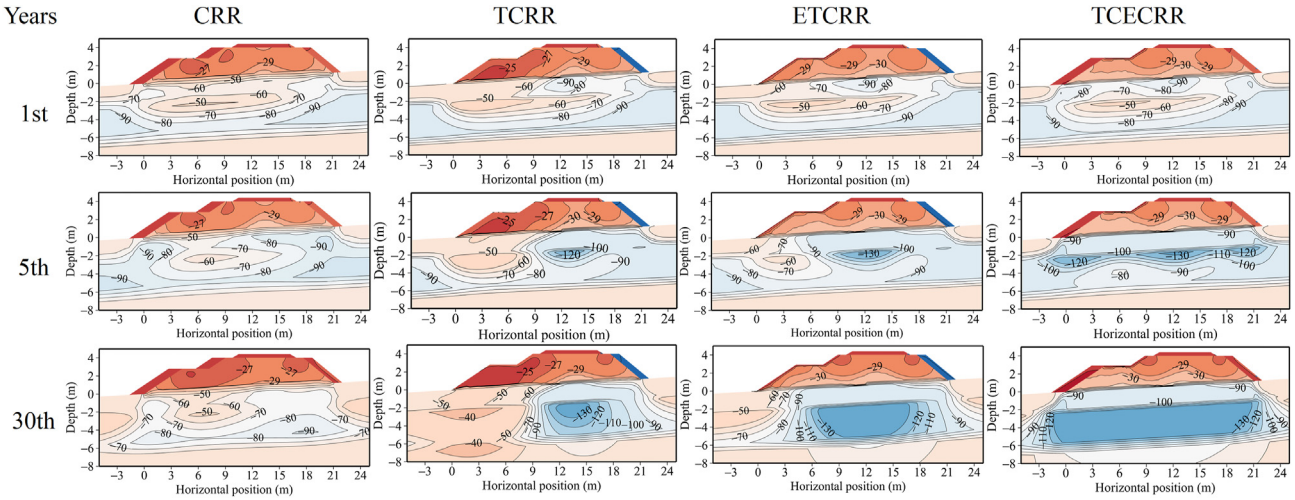

Fig. 10. Enthalpy of the reinforced embankment on 15 October the in the 1st, 5th and 30th year.

RTCRR and TCECRR. In general, the surface heat flux of the evaporation section of the TPCT is decreasing year by year under the three working conditions. After TCRR strengthening, in the above three years, the heat flux value in the soil layer below −6 m is higher than the other two. However, within the range of 0–6 m, the heat flux value decreases rapidly in the direction close to the top of the evaporation section, and is obviously smaller than the other two schemes within the range of 0–4 m. The heat flux distribution curves of ETCRR and TCECRR are similar, but the heat flux of ETCRR scheme in the same year and location is greater than that of TCECRR. The difference between them gradually increases towards the upper part of the evaporation section. In addition, the difference is increasing with year.

Fig. 14 shows the heat flux time history curves in the 1st, 5th and 30th years for the heat flux at the positions 1/4, 1/2, 3/4 and 4/4 from the top of the evaporation section of the TPCT in the three schemes of TCRR, ETCRR and TCECRR. On the whole, the heat flux evolution trend at different positions of the evaporation section of the TPCT in the ETCRR enhancement scheme is basically similar to that in the TCECRR. According to the annual change of heat flux at the 1/4–1/2 evaporation section length from the top down in Fig. 14a and b, the start time of the TPCTs in TCRR scheme is obviously earlier than that in the other two schemes, but the stop time is later than that in the other two schemes. Atthe same time, in this range, the maximum power (maximum heat flux) of the TPCT in TCRR is also smaller than that of the other two cases, and its corresponding time is also earlier than that of the other two cases. This shows that although the thermal protection measures on the surface of the sunny slope subgrade in the ETCRR and TCECRR schemes hinder the natural refreezing process of the underlying soil layer to some extent, this effect ensures the temperature difference between the soil layer and the outside atmosphere within the range, and enhances the working efficiency of the TPCT. From Figs. 7, 10 and 12, the ETCRR and TCECRR schemes show noticeable and powerful thermal insulation advantages during the shutdown period of TPCTs in the warm season. In combination with Figs. 6 and 8, the above process makes the comprehensive cooling effect of ETCRR and TCECRR schemes stronger than that of TCRR. According to the change of heat flux from the 3/4 evaporation section length to the bottom of the TPCT (Fig. 14a), the heat flux of the evaporation section wall in the TCRR scheme becomes greater than that in the other two schemes over time. In combination with Figs. 6, 8 and 9, this is mainly due to the poor comprehensive cooling effect of TCRR, which leads to the temperature increase of deep frozen soil in the medium and long term, and expands the temperature difference between deep frozen soil and the outside atmosphere in cold season. Compared with the ETCRR and TCECRR schemes, the heat flux at almost any position in the evaporation section of the ETCRR scheme is slightly greater than that of the TCECRR scheme, and this gap also expands slightly over time.

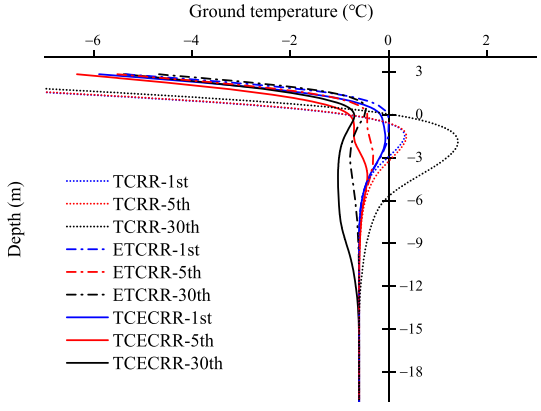

Fig. 11. Calculation results of ground temperature–depth curve on 15 January at the step center on the sunny slope.

4.3. Economical applicability analysis

The above results show that the composite reinforcements can dramatically cool the permafrost foundation, uplift PT,

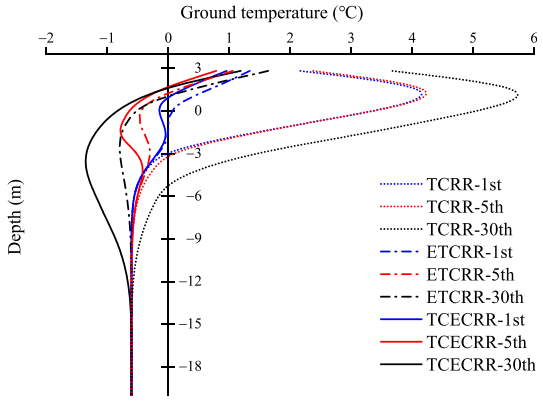

Fig. 12. Calculation results of ground temperature–depth curve on 15 October at the step center on the sunny slope.

and improve its long-term thermal stability. Although TCRR scheme can cool the soil mass below the central embankment, the permafrost under the sunny slope is still continuous degenerating, and potentially threatens stability of subgrade slope. So, it is not recommended using as a reinforcement measure. ETCRR and TCECRR schemes have better cooling capacity throughout the service life and can be used as alternative reinforcement measures. However, to judge whether the reinforcement measures are applicable to the actual project, it is necessary to evaluate their economic rationality. We investigated the current cost of materials, labor and transportation in the market of China, and found that the purchase cost of glass fiber grating and TPCT in ETCRR and TCECRR schemes is about 3.53 times and 3.51 times of that in CRR schemes, respectively, if estimated by the reinforcement length of 100 m. However, considering the construction efficiency and other factors, the labor cost of ETCRR and TCECRR is only 20% and 60% of that of CRR. For the transportation cost, we estimated it according to the truck with a load of 25 t and a capacity of 60 m^3. The transportation costs of ETCRR and TCECRR are relatively low, only 6.4% and 72.4% of CRR respectively. In terms of

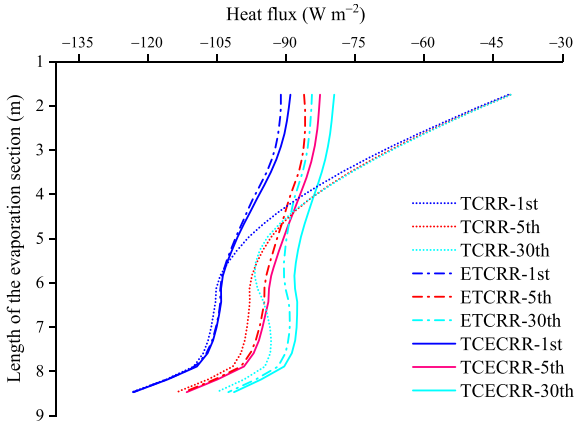

Fig. 13. Simulation results of the transient heat flow distribution curve of evaporation section pipe wall on 15 January, in the 1st, 5th and 30th years in TCRR, ETCRR and TCECRR schemes.

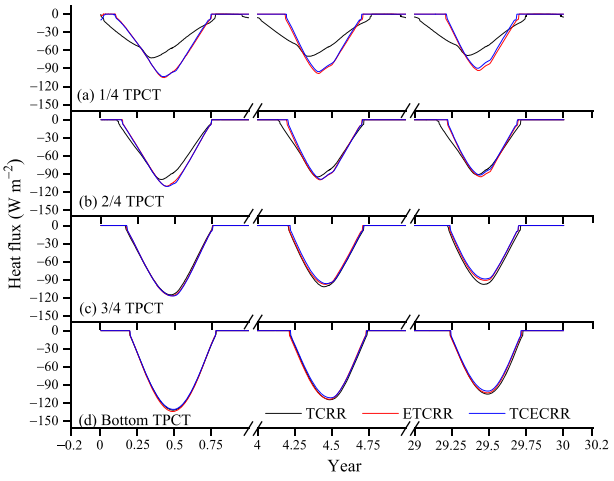

Fig. 14. Simulation results of heat flux time history curve at different positions of TPCT evaporation section in TCRR, ETCRR and TCECRR schemes.

overall cost, compared with CRR scheme, ETCRR scheme can save 52.1% of the cost, while TCECRR scheme can only save 1% of the cost. It can be seen that under the condition of sufficient project budget, using TCECRR scheme can achieve more efficient cooling process and ensure the long-term stability of high-temperature permafrost foundation. If the project budget is tight, ETCRR can also be strengthened. However, from the perspective of Figs. 6 and 7, the project maintenance cost in 0–5 years after using this scheme may be higher than that of TCECRR.

4.4. Improvement, limitation and uncertainty

The disposal measures studied here are all proposed to precisely solve the differential degradation problem of permafrost foundation on the lower part of shady slope and sunny slope of railway embankment under the action of climate warming and engineering disturbance. The strengthening measures for the sections with perennial surface runoff, the transition sections of roads and bridges, and the sections with strong heat and melt disasters are still very complex and requires further research. The numerical model used involves the coupled heat transfer process of TPCTs and crushed rock applied in the embankment. Among them, the model for calculating heat transfer in TPCTs has been successfully applied in other literature (Pei et al., 2019a, 2019b). The calculation results of the model considering local non thermal equilibrium heat transfer in the crushed/ripped rock layer have also been confirmed in our other article to be superior to the calculation results under the assumption of local thermal equilibrium (Hou et al., 2022b). Therefore, due to space limitations, this study did not further validate the calculation results.

5. Conclusion

(1) When the traditional crushed rock revetment is used to reinforce the general embankment on both the shady and

sunny embankment slopes, it can only limit the temperature increasing process of the underlying permafrost, which is not enough to completely eliminate the warm permafrost areas formed during the previously operation.

(2) When the TCRR scheme is adopted, although the cooling effect is apparently adjacent to the shady side, the permafrost deteriorating directly below the sunny slope is still ongoing. This may lead to thermal slippage in the corresponding locations.

(3) When ETCRR and TCECRR schemes are implemented, the thermal field for the permafrost foundation can be relatively comprehensively 'repaired' and further cooled. Nevertheless, either from the perspective of working efficiency or the effective range in the above process, TCECRR scheme is notably superior to the former.

(4) The thermal insulation material laid in the ETCRR and TCECRR schemes retards the natural refreezing and cooling process of the soil layer below, but improve the working intensity of the TPCTs because the temperature difference between the evaporation section and the external environment is accordingly maintained in the early cold season. In addition, the thermal insulation material can well isolate the heat input in warm season. Therefore, the thermal insulation material further improves the comprehensive cold energy storing capacity of TCRR.

(5) Among TCECRR scheme, the crushed rock laid on the lower steps of the sunny slope has further improved the overall working efficiency of the composite strengthening measures due to its 'thermal semiconductor' effect, and homogenizes the thermal field under the embankment in the horizontally direction.

Declaration of competing interest

The authors declare no conflict of interest.

Acknowledgments

This research was funded by National Natural Science Foundation of China (41861010, 41801033), The CAS Light of the West China Training Program (Granted to Dr. Yan-Dong Hou), the Funds for Creative Research Groups of Gansu Province, China (20JR5RA478), Science and Technology Program of Gansu Province (22YF11GA302).

Appendix A. Supplementary data

Supplementary data to this article can be found online at https://doi.org/10.1016/j.accre.2023.05.007.

References

Chen, L., Yu, W.B., Lu, Y., et al., 2018. Numerical simulation on the performance of thermosyphon adopted to mitigate thaw settlement of embankment in sandy permafrost zone. Appl. Therm. Eng. 128, 1624−1633. https://doi.org/10.1016/j.applthermaleng.2017.09.130.

Hou, Y.D., Wu, Q.B., Wang, K.G., et al., 2020. Numerical evaluation for protecting and reinforcing effect of a new designed crushed rock revetment on Qinghai−Tibet Railway. Renew. Energy 156, 645−654. https://doi.org/10.1016/j.renene.2020.04.066.

Hou, Y.D., Wu, Q.B., Zhang, M.L., et al., 2022a. Thermal and deformational repairing effect of crushed rock revetment acting as reinforcement along Qinghai−Tibet Railway in permafrost regions. Adv. Clim. Change Res. 13, 421−431. https://doi.org/10.1016/j.accre.2022.03.001.

Hou, Y.D., Wang, K.G., Lei, W.Y., et al., 2022b. Research local thermal non-equilibrium effect in crushed rock based embankment. J. Glaciol. Geocryol. 44, 1−13. https://kns.cnki.net/kcms/detail/62.1072.P.20220721.1632.008.html.

Hou, Y.D., Wu, Q.B., Dong, J.H., et al., 2018. Numerical simulation of efficient cooling by coupled RR and TCPT on railway embankments in permafrost regions. Appl. Therm. Eng. 133, 351−360. https://doi.org/10.1016/j.applthermaleng.2018.01.070.

Jiang, P.X., Ren, Z.P., Wang, B.X., et al., 1996. Forced convective heat transfer in a plate channel filled with solid particles. J. Therm. Sci. 5 (1), 43−53. https://kns.cnki.net/KCMS/detail/detail.aspx?dbcode=CJFD&dbname=CJFD9697&filename=RKXY601.008.

Li, S.Y., Niu, F.J., Lai, Y.M., et al., 2017. Optimal design of thermal insulation layer of a tunnel in permafrost regions based on coupled heat−water simulation. Appl. Therm. Eng. 110, 1264−1273. https://doi.org/10.1016/j.applthermaleng.2016.09.033.

Liu, M.H., Li, G.Y., Niu, F.J., et al., 2017. Porosity of crushed rock layer and its impact on thermal regime of Qinghai−Tibet Railway embankment. J. Cent. South Univ. 24, 977−987. https://doi.org/10.1007/s11771-017-3500-2.

Ma, W., Wen, Z., Sheng, Y., et al., 2012. Remedying embankment thaw settlement in a warm permafrost region with thermosyphons and crushed rock revetment. Can. Geotech. J. 49, 1005−1014. https://doi.org/10.1139/t2012-058.

Mu, Y.H., Ma, W., Wu, Q.B., et al., 2012. Cooling processes and effects of crushed rock embankment along the Qinghai−Tibet Railway in permafrost regions. Cold Reg. Sci. Technol. 78, 107−114. https://doi.org/10.1016/j.coldregions.2012.01.014.

Mu, Y.H., Ma, W., Li, G.Y., et al., 2018. Impacts of supra-permafrost water ponding and drainage on a railway embankment in continuous permafrost zone, the interior of the Qinghai−Tibet Plateau. Cold Reg. Sci. Technol. 154, 23−31. https://doi.org/10.1016/j.coldregions.2018.06.007.

Niu, F.J., Lin, Z.J., Lu, J.H., et al., 2011. Characteristics of roadbed settlement in embankment−bridge transition section along the Qinghai−Tibet Railway in permafrost regions. Cold Reg. Sci. Technol. 65, 437−445. https://doi.org/10.1016/j.coldregions.2010.10.014.

Pei, W.S., Zhang, M.Y., Li, S.Y., et al., 2017. Thermo-mechanical stability analysis of cooling embankment with crushed-rock interlayer on a sloping ground in permafrost regions. Appl. Therm. Eng. 125, 1200−1208. https://doi.org/10.1016/j.applthermaleng.2017.07.105.

Pei, W.S., Zhang, M.Y., Lai, Y.M., et al., 2019a. Evaluation of the ground heat control capacity of a novel air-L-shaped TPCT-ground (ALTG) cooling system in cold regions. Energy 179, 655−668. https://doi.org/10.1016/j.energy.2019.04.156.

Pei, W.S., Zhang, M.Y., Yan, Z.R., et al., 2019b. Numerical evaluation of the cooling performance of a composite L-shaped two-phase closed thermosyphon (LTPCT) technique in permafrost regions. Sol. Energy 177, 22−31. https://doi.org/10.1016/j.solener.2018.11.001.

Pei, W.S., Zhang, M.Y., Wan, X.S., et al., 2021. Numerical optimization of the installing position for the L-shaped TPCT in a permafrost embankment based on the spatial heat control. Sol. Energy 224, 1406−1425. https://doi.org/10.1016/j.solener.2021.06.044.

Peng, E.X., Hu, X.Y., Sheng, Y., et al., 2022. Thermal effect of the accumulated water with different depths on permafrost subgrade in cold regions. Adv. Clim. Change Res. 1−12. https://doi.org/10.1016/j.accre.2022.08.003.

Qin, Y.H., Zhang, J.M., 2010. Estimating the stability of unprotected embankment in warm and ice-rich permafrost region. Cold Reg. Sci. Technol. 61, 65−71. https://doi.org/10.1016/j.coldregions.2009.12.001.

Sun, Z.Z., Ma, W., Zhang, S.J., et al., 2018. Characteristics of thawed interlayer and its effect on embankment settlement along the Qinghai−Tibet Railway in permafrost regions. J. Mt. Sci. 15, 1090−1100. https://doi.org/10.1007/s11629-017-4643-1.

Wang, H.L., Sun, Z.Z., Liu, Y.Z., et al., 2018. Thermal state of embankment with thawed interlayer in permafrost regions of the Qinghai−Tibet Railway. J. Glaciol. Geocryol. 40, 934−942. https://doi.org/10.7522/j.issn.1000-0240.2018.0508.

Wang, H.L., Sun, Z.Z., Liu, M.H., et al., 2021. Improvement of the thermo-mechanical stability of an embankment with suprapermafrost taliks by engineering remedial countermeasures. J. Cold Reg. Eng. 35, 1−8. https://doi.org/10.1061/(asce)cr.1943-5495.0000269.

Wen, Z., Sheng, Y., Ma, W., et al., 2010. Probabilistic analysis of the replacement thickness of the in-cuts roadbed in permafrost regions. Cold Reg. Sci. Technol. 64, 57−67. https://doi.org/10.1016/j.coldregions.2010.07.002.

Wu, Q.B., Liu, Y.Z., Zhang, J.M., et al., 2002. A review of recent frozen soil engineering in permafrost regions along Qinghai−Tibet Highway, China. Permafr. Periglac. Process. 13, 199−205. https://doi.org/10.1002/ppp.420.

Wu, Q.B., Zhao, H.T., Zhang, Z.Q., et al., 2020. Long-term role of cooling the underlying permafrost of the crushed rock structure embankment along the Qinghai−Xizang Railway. Permafr. Periglac. Process. 31, 172−183. https://doi.org/10.1002/ppp.2027.

Xu, Y.Z., Shen, M.D., Zhou, Z.W., et al., 2022. Long-term thermal stability study of the typical embankment along the Qinghai−Tibet Railway in warm permafrost regions. J. Glaciol. Geocryol. 44 (6), 1−12. https://kns.cnki.net/kcms/detail/62.1072.P.20221108.1403.004.html.

Yan, Z.R., Zhang, M.Y., Lai, Y.M., et al., 2020. Countermeasures combined with thermosyphons against the thermal instability of high-grade highways in permafrost regions. Int. Commun. Heat Mass Tran. 153, 1−15. https://doi.org/10.1016/j.ijheatmasstransfer.2019.119047.

Yu, F., Zhang, M.Y., Lai, Y.M., et al., 2017. Crack formation of a highway embankment installed with two-phase closed thermosyphons in permafrost regions: field experiment and geothermal modelling. Appl. Therm. Eng. 115, 670−681. https://doi.org/10.1016/j.applthermaleng.2017.01.001.

Zhang, M.Y., Lai, Y.M., Dong, Y.H., 2009. Numerical study on temperature characteristics of expressway embankment with crushed-rock revetment and ventilated ducts in warm permafrost regions. Cold Reg. Sci. Technol. 59, 19−24. https://doi.org/10.1016/j.coldregions.2009.06.001.

Zhang, M.Y., Lai, Y.M., Zhang, J.M., et al., 2011. Numerical study on cooling characteristics of two-phase closed thermosyphon embankment in permafrost regions. Cold Reg. Sci. Technol. 65, 203−210. https://doi.org/10.1016/j.coldregions.2010.08.001.

Zhang, M.Y., Pei, W.S., Zhang, X.Y., et al., 2015. Lateral thermal disturbance of embankments in the permafrost regions of the Qinghai−Tibet engineering corridor. Nat. Hazards 78, 2121−2142. https://doi.org/10.1007/s11069-015-1823-6.

Zhang, M.Y., Pei, W.S., Lai, Y.M., et al., 2017a. Numerical study of the thermal characteristics of a shallow tunnel section with a two-phase closed thermosyphon group in a permafrost region under climate warming. Int. Commun. Heat Mass Transfer 104, 952−963. https://doi.org/10.1016/j.ijheatmasstransfer.2016.09.010.

Zhang, M.Y., Pei, W.S., Li, S.Y., et al., 2017b. Experimental and numerical analyses of the thermo-mechanical stability of an embankment with shady and sunny slopes in a permafrost region. Appl. Therm. Eng. 127, 1478−1487. https://doi.org/10.1016/j.applthermaleng.2017.08.074.

Zhao, H.T., Wu, Q.B., Zhang, Z.Q., 2019. Long-term cooling effect of the crushed rock structure embankments of the Qinghai−Tibet Railway. Cold Reg. Sci. Technol. 160, 21−30. https://doi.org/10.1016/j.coldregions.2019.01.006.